

Magnetic phase transitions, magnetocrystalline anisotropy, and crystal-field interactions in the $R\text{Fe}_{11}\text{Ti}$ series (where $R = \text{Y, Pr, Nd, Sm, Gd, Tb, Dy, Ho, Er, or Tm}$)

X. C. Kou,* T. S. Zhao,[†] R. Grössinger, and H. R. Kirchmayr

Institute for Experimental Physics, Technical University of Vienna, A-1040 Vienna, Austria

X. Li and F. R. de Boer

Van der Waals-Zeeman Laboratory, University of Amsterdam, 1018 XE Amsterdam, The Netherlands

(Received 21 July 1992)

A systematic investigation of the intrinsic magnetic properties of $R\text{Fe}_{11}\text{Ti}$ compounds with $R = \text{Y, Pr, Nd, Sm, Gd, Tb, Dy, Ho, Er, and Tm}$ has been performed by means of ac susceptibility measurements, singular-point-detection techniques, and high-field magnetization measurements. Spin-reorientation transitions were observed in $R\text{Fe}_{11}\text{Ti}$ with $R = \text{Nd}$ ($T_{\text{SR}} = 189 \text{ K}$), Tb ($T_{\text{SR}} = 339 \text{ K}$), Dy ($T_{\text{SR1}} = 214 \text{ K}$ and $T_{\text{SR2}} = 98 \text{ K}$), and Er ($T_{\text{SR}} = 48 \text{ K}$). First-order magnetization processes of type I for $R = \text{Nd}$ and Er and of type II for $R = \text{Ho}$ and Tm were detected at low temperatures. The uniaxial magnetocrystalline anisotropy fields of the whole $R\text{Fe}_{11}\text{Ti}$ series have been determined in a wide temperature interval from 4.2 K to the Curie temperatures. It is deduced that the "anomalous increase" in the magnetization curve of $\text{SmFe}_{11}\text{Ti}$ for the external field perpendicular to the c axis is not a first-order magnetization process, but a continuous rotation of the magnetic moment under the action of the external field. The observed magnetic phase transitions, the spin-reorientation transitions, and the first-order magnetization processes in the $R\text{Fe}_{11}\text{Ti}$ compounds are well described in terms of a crystal-field description in which the rare-earth sublattice (R) and transition-metal sublattice (T) exchange interaction is included. A set of crystalline-electric-field parameters as well as the values for the R - T exchange field are deduced for the whole $R\text{Fe}_{11}\text{Ti}$ series from fitting the experimentally obtained values of the anisotropy field, the critical field for the first-order magnetization process, and the spin-reorientation temperature with the calculations in the present systematic study. Magnetic anomalies are observed in the temperature dependence of the ac susceptibility of the $R\text{Fe}_{11}\text{Ti}$ compounds with $R = \text{Nd, Sm, Er, and Tm}$. They are shown to be connected with domain-wall motion.

I. INTRODUCTION

After the discovery of permanent magnets based on the ternary compound $\text{Nd}_2\text{Fe}_{14}\text{B}$, the recent trend in the search for new magnetic materials has turned to ternary systems of the types rare-earth-transition-metal-metalloid or rare-earth-transition-metal-transition-metal. Among these systems the $R(\text{Fe,Ti})_{12}$ series has attracted considerable attention.

Many investigations of the intrinsic magnetic properties of $R(\text{Fe,Ti})_{12}$ compounds have been reported, mostly on polycrystalline samples, but also in some cases on single crystals e.g., of the compounds with $R = \text{Sm}$,¹⁻³ Dy ,^{4,5} Er , and Lu .⁶ The $R\text{Fe}_{11}\text{Ti}$ compounds crystallize in the tetragonal structure with the space group of $14/mmm$.⁷ In this structure, the rare-earth ion occupies the $2a$ crystallographic site, and the Fe and Ti ions preferentially occupy three crystallographically inequivalent sites, the $8i$, $8j$, and $8f$ sites. The $8j$ and $8f$ sites are almost fully occupied by Fe ions.⁸ Therefore, the $R\text{Fe}_{11}\text{Ti}$ compounds can be regarded as ternary compounds.

Considerable confusion exists about the types of magnetic structures occurring in the various $R\text{Fe}_{11}\text{Ti}$ compounds at various temperatures and about the nature of the field-induced magnetic phase transitions. In the present paper, a systematic investigation of the

temperature- and field-induced magnetic phase transitions in $R\text{Fe}_{11}\text{Ti}$ compounds is presented. Particular attention is given to the study of the temperature dependence of the magnetocrystalline anisotropy, which hitherto has not been studied in much detail.

From the application point of view, the $R\text{Fe}_{11}\text{Ti}$ system is not very promising. Only the Sm compound has strong uniaxial anisotropy. However, the coercivity realized is, so far, disappointing.^{9,10} From a fundamental point of view, this series provides a very nice opportunity to study the crystalline-electric-field (CEF) effect in R - T intermetallic compounds. The reasons are as follows. Firstly, the contribution to the net anisotropy of $R\text{Fe}_{11}\text{Ti}$ from the Fe sublattice favors the c axis and the value is large. Secondly, there is only one rare-earth site in the ThMn_{12} structure, which provides the simplest case of the CEF effects on the rare-earth ion. Thirdly, the contribution to the net anisotropy of $R\text{Fe}_{11}\text{Ti}$ from the R sublattice is not completely predictable if we only take into account the second-order CEF term. The contribution to the net anisotropy from the fourth-order as well as the sixth-order CEF terms is significant. From the CEF calculation it follows that the fourth-order or sixth-order CEF terms lead to easy magnetization directions (EMD) that deviate from the c axis. Therefore, temperature-induced magnetic-phase transitions, like spin reorienta-

tions or anomalous magnetic processes, e.g., FOMP's, are expected to occur in these compounds. The occurrence of these transitions poses strong limitations on the values of the CEF parameters. Therefore, a reliable set of the CEF parameters and R - T exchange fields can be derived by fitting the experiments with CEF calculations.

The present paper is organized as follows. In Sec. II the experimental procedures are described in detail. In Sec. III the details are given of the CEF calculations in which the combined interaction of the crystalline electric field and the R - T exchange field has been taken into account. In Sec. IV the experimental and the calculation results are presented. Each compound is discussed separately. A summary and some general conclusions are presented in Sec. V.

II. EXPERIMENTAL DETAILS

Polycrystalline $R\text{Fe}_{11}\text{Ti}$ ingots with $R = \text{Y, Pr, Nd, Sm, Gd, Tb, Dy, Ho, Er, and Tm}$ were prepared by induction melting of appropriate amounts of the starting materials of at least 99.9 wt % purity. The ingots were remelted at least four times in order to achieve homogeneity. Weight losses during the melting due to evaporation of the rare-earth element were compensated by starting with an excess of 3 wt % R (with respect to the R content). The ingots were wrapped in Mo foil and sealed in quartz tubes filled with helium gas after having been evacuated. Subsequently, the compounds with $R = \text{Y, Gd, Dy, Tb, Ho, Er, and Tm}$ were annealed at 1173 K for three weeks. The compounds with $R = \text{Pr, Nd, and Sm}$ were annealed at 1373 K for three weeks. In order to avoid possible crystallographic phase transitions during the cooling, the samples were water quenched. The annealed samples were checked by x-ray diffraction and optical microscopy. It was found that all the samples are single phase with the expected tetragonal structure, except $\text{PrFe}_{11}\text{Ti}$, which contains a few percent Fe and Fe_2Ti as impurity phases. The lattice constants a and c were determined from the x-ray diffraction patterns by means of the [301], [002], [222], [312], [510], [422] reflections (Fig. 1). Magnetically aligned samples were prepared by fixing powder particles aligned at room temperature in a

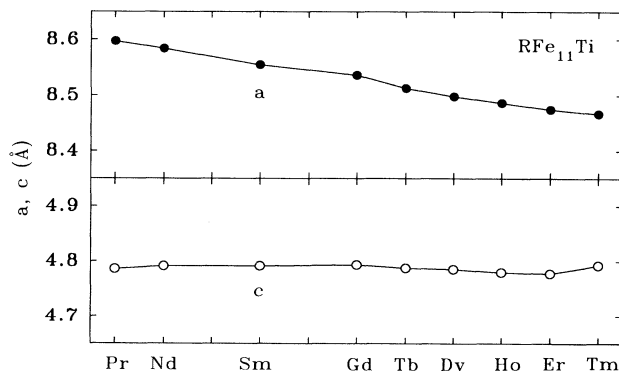


FIG. 1. Lattice constants a and c of $R\text{Fe}_{11}\text{Ti}$ compounds.

field of 1 T with a resin-doped epoxy solution.

The temperature dependences of the real component (χ') and the imaginary component (χ'') of the ac susceptibility were measured in order to determine the onset temperatures of the magnetic phase transitions. These measurements allow an unambiguous determination of the onset temperature of the magnetic phase transition caused by the change of the anisotropy energy. For highly anisotropic materials like the $R\text{Fe}_{11}\text{Ti}$ compounds, the value of χ' is mainly determined by the magnetic anisotropy energy and the domain-wall energy. The value of χ'' reflects the energy absorption by the sample, which mainly arises from the domain-wall movement. In these compounds, the energy absorption due to eddy currents is negligible. An ac susceptometer (Lake Shore, model 7000) was used, which can be operated in the temperature range 4.2–300 K with ac fields from 0.4 to 800 A/m and frequencies from 5 to 1000 Hz. In the present investigation, a field of 40 A/m and a frequency of 1000 Hz were used. The onset temperature of a first-order magnetic phase transition is reflected as a kink in the χ' vs the T curve. In the case of a second-order magnetic phase transition, the onset temperature can be identified as the temperature where $d\chi'/dT$ achieves a minimum. Above 300 K, the spin-reorientation transitions in $R\text{Fe}_{11}\text{Ti}$ compounds were detected by measurement of the temperature dependence of the magnetization in a Foner vibrating-sample magnetometer.

The anisotropy fields of the bulk polycrystalline samples were determined by means of the singular-point-detection (SPD) technique.^{11–14} This method was also used to determine the critical field of the first-order magnetization process (FOMP).^{14–16} The measurements were performed in a pulsed-field facility, which is divided into two subsystems. One system can be operated from 4.2 to 300 K with a maximum field of 30 T. The measurements in this system were carried out with decreasing temperature on aligned samples with the field applied perpendicular to the alignment direction. The other system can be operated from 300 to 1000 K with a maximum field of 28 T. The measurements in this system were carried out on polycrystalline material. The system was calibrated with a spherical single crystal of Ba ferrite, which has an anisotropy field of 1.68 T and a saturation magnetization of 1.48 T.¹⁷

The magnetization in very high fields was measured at 4.2 K in the Amsterdam High-Field Installation in which semicontinuous fields up to 40 T can be generated.^{18–20}

III. METHOD OF CALCULATION

In the presence of an external field \mathbf{B} , the Hamiltonian of the magnetic R ion in $R\text{Fe}_{11}\text{Ti}$ compounds can be expressed as

$$\mathcal{H} = \lambda \mathbf{L} \cdot \mathbf{S} + \mathcal{H}_{\text{CEF}} + 2\mu_B \mathbf{S} \cdot \mathbf{B}_{\text{exch}} + \mu_B (\mathbf{L} + 2\mathbf{S}) \cdot \mathbf{B}, \quad (1)$$

where λ is the spin-orbit coupling constant; \mathbf{L} and \mathbf{S} are the total orbital and spin angular momenta, respectively; μ_B is the Bohr magneton; \mathbf{B}_{exch} is the exchange field due to the Fe sublattice acting on the $4f$ spin. \mathcal{H}_{CEF} represents the crystal-field Hamiltonian which in the

tetragonal symmetry of the ThMn_{12} structure can be written as

$$\mathcal{H}_{\text{CEF}} = A_2^0 C_2^0 + A_4^0 C_4^0 + A_4^4 (C_4^4 + C_4^{-4}) + A_6^0 C_6^0 + A_6^4 (C_6^4 + C_6^{-4}), \quad (2)$$

where A_n^m and C_n^m are the CEF parameters and the tensor operators, respectively.

The matrix elements of Eq. (1) have been calculated by means of the irreducible tensor operator technique.²¹ For a given applied field \mathbf{B} and a direction of \mathbf{B}_{exch} , the eigenvalues E_n and eigenfunctions $|n\rangle$ [$n=1, 2, \dots, \sum_J (2J+1)$] are obtained by diagonalizing the $\sum_J (2J+1) \times \sum_J (2J+1)$ matrix of Eq. (1). The diagonalization is carried out within the subspace of only the ground-state J multiplet for the heavy- R ions, and within the subspace consisting of the ground-state and the first excited-state J multiplets for the Pr and Nd ions with $\lambda=620$ and 536 K, respectively, and within the subspace consisting of the ground-state and the two lowest excited-state J multiplets for the Sm ion with $\lambda=410$ K. The free energy is given by

$$F(T, \mathbf{B}, \mathbf{B}_{\text{exch}}) = -k_B T \ln Z + \mathbf{K}_1^{\text{Fe}} \sin^2 \theta_{\text{Fe}} - \mathbf{M}_{\text{Fe}} \cdot \mathbf{B}, \quad (3)$$

$$Z = \sum_n \exp(-E_n/k_B T), \quad (4)$$

where \mathbf{K}_1^{Fe} and \mathbf{M}_{Fe} are the magnetic anisotropy constant and the magnetic moment of the Fe sublattice per formula unit, respectively. $\mathbf{B}_{\text{exch}}(T)$ is assumed to be proportional to and is antiparallel to $\mathbf{M}_{\text{Fe}}(T)$. The values of $\mathbf{K}_1^{\text{Fe}}(T)$ and $\mathbf{M}_{\text{Fe}}(T)/\mathbf{M}_{\text{Fe}}(0)$ are assumed to be the same as those in YFe_{11}Ti after scaling the different Curie temperatures. The values of \mathbf{K}_1^{Fe} for YFe_{11}Ti at various temperatures were deduced from the formula $\mathbf{K}_1^{\text{Fe}} = \mathbf{M}_{\text{Fe}} \mathbf{B}_a / 2$, whereas the values of \mathbf{B}_a were determined by the SPD technique after correcting for the demagnetization field (Fig. 2). The obtained value of \mathbf{K}_1^{Fe} is 23.2 K/f.u. at 4.2 K. The experimental values for \mathbf{M}_{Fe} in YFe_{11}Ti at various temperatures were taken from the literature.²²

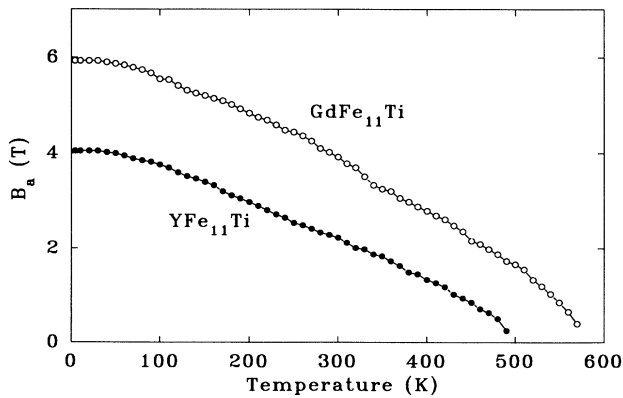


FIG. 2. Temperature dependence of the anisotropy field B_a of YFe_{11}Ti (●) and $\text{GdFe}_{11}\text{Ti}$ (○) determined by the SPD technique.

The equilibrium direction of \mathbf{M}_{Fe} , for given applied field \mathbf{B} and temperature T , can be determined by minimizing the free energy $F(T, \mathbf{B}, \mathbf{B}_{\text{exch}})$. The magnetic moment of the R ion is given by

$$\mathbf{M}_R(T) = \sum_n -\mu_B \langle n | (\mathbf{L} + 2\mathbf{S}) | n \rangle \frac{\exp(-E_n/k_B T)}{Z}, \quad (5)$$

The total magnetization of the $R\text{Fe}_{11}\text{Ti}$ compound is given by

$$\mathbf{M}(T, \mathbf{B}) = \mathbf{M}_R(T) + \mathbf{M}_{\text{Fe}}(T). \quad (6)$$

It should be noted that the calculation method described above has been used by many researchers in calculating the magnetization curves of rare-earth compounds, as e.g., by Hu *et al.*,⁵ Li *et al.*,²⁶ and Moze *et al.*²⁹ in $R(\text{Fe}, \text{Ti})_{12}$ compounds and Yamada *et al.*³¹ in $R_2\text{Fe}_{14}\text{B}$ compounds.

From the above description it follows that the $\mathbf{M}(T, \mathbf{B})$ curves along different crystallographic directions can be calculated if the values of the CEF parameters A_n^m and the R - T exchange field \mathbf{B}_{exch} are known. In the present paper, a set of A_n^m and \mathbf{B}_{exch} values has been determined by fitting the calculations to the experimental data. In doing this, with only data on polycrystalline samples being available, particular emphasis has been given to fit the calculations to the experimental values for the anisotropy field B_a , the critical field of the FOMP B_{cr} and spin-reorientation temperature T_{SR} .

IV. RESULTS AND DISCUSSION

In the R - T intermetallic compounds, the contribution to the net anisotropy from the R sublattice generally dominates at lower temperatures, whereas the T -sublattice anisotropy dominates at high temperatures. Also, the R -sublattice anisotropy decreases much faster with increasing temperature than the T -sublattice anisotropy. In $R\text{Fe}_{11}\text{Ti}$ compounds, the Fe-sublattice anisotropy favors the c axis at all temperatures up to the Curie temperature. The easy magnetization direction (EMD) of the R sublattice depends on the CEF interaction and the exchange field experienced by the R ion. If we consider only the second-order CEF term, it can be deduced that the Sm, Er, and Tm sublattices have a uniaxial contribution to the net anisotropy, whereas the remaining magnetic R ions have planar contributions to the net anisotropy. Therefore, many temperature-induced changes of the EMD are expected in $R\text{Fe}_{11}\text{Ti}$, either due to the temperature-induced competition between the R - and the Fe-sublattice anisotropies or due to temperature-induced changes in the R -sublattice anisotropy only.

A. YFe_{11}Ti and $\text{GdFe}_{11}\text{Ti}$

The compounds YFe_{11}Ti and $\text{GdFe}_{11}\text{Ti}$ exhibit very similar anisotropy behavior, because Y is nonmagnetic and Gd is an S -state ion. Therefore, these two compounds can be considered as pure “ $3d$ compounds”, in which only the Fe sublattice contributes to the anisotropy. Both compounds, YFe_{11}Ti and $\text{GdFe}_{11}\text{Ti}$, are report-

ed to exhibit uniaxial anisotropy.²² The temperature dependence of the anisotropy field B_a and anisotropy constant K_1 of YFe_{11}Ti has been determined by Moze *et al.*⁸ and Coey²³ in the temperature range 77–300 K.

The temperature dependence of the ac susceptibility of YFe_{11}Ti and $\text{GdFe}_{11}\text{Ti}$ as investigated in the present study does not show any anomaly between 4.2 and 300 K, suggesting that the EMD of the $3d$ -sublattice magnetization remains unchanged in this temperature range. Figure 2 shows the temperature dependence of the anisotropy field for YFe_{11}Ti and $\text{GdFe}_{11}\text{Ti}$ as determined by the SPD technique. These measurements confirm that the EMD in these compounds is along the c axis, and show this to be the case up to the magnetic ordering temperature.

B. $\text{PrFe}_{11}\text{Ti}$

Due to the difficulty in preparing $\text{PrFe}_{11}\text{Ti}$ with the tetragonal ThMn_{12} structure, not many reports on the magnetic properties of $\text{PrFe}_{11}\text{Ti}$ are available in the literature. The EMD of $\text{PrFe}_{11}\text{Ti}$ at room temperature has been determined to be within the basal plane by means of x-ray diffraction on a magnetically aligned sample and a Curie temperature of 530 K has been reported.²⁴ This means that at room temperature the Pr-sublattice anisotropy dominates the uniaxial Fe-sublattice anisotropy.

In the present study, it was found that by annealing for three weeks at 1373 K almost single-phase $\text{PrFe}_{11}\text{Ti}$ with the tetragonal ThMn_{12} structure could be prepared with only a few percent of Fe_2Ti and Fe as impurity phases. The temperature dependence of the ac susceptibility shown in Fig. 3 does not reveal any anomaly between 4.2 and 300 K, suggesting that the EMD of $\text{PrFe}_{11}\text{Ti}$ remains within the basal plane in this temperature interval. However, it can be expected that the planar Pr-sublattice anisotropy decreases much faster with increasing temperature than the uniaxial Fe-sublattice anisotropy. Therefore, a spin-reorientation transition from the basal plane to the c axis may be expected above room temperature. In order to investigate this, the temperature dependence of the magnetization was measured from 4.2 up to 800 K in a low external field of 0.005 T. However, no spin reorientation could be detected, indicating that the planar anisotropy of the Pr sublattice dominates the uniaxial anisotropy of the Fe sublattice up to the Curie temperature.

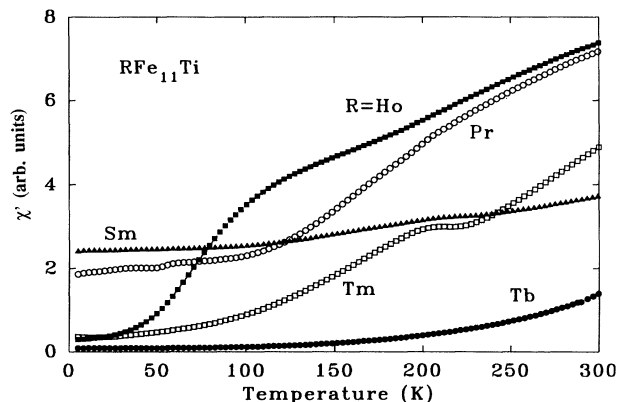


FIG. 3. Temperature dependence of χ' of RFe_{11}Ti with $R = \text{Pr}(\circ)$, $\text{Sm}(\blacktriangle)$, $\text{Tb}(\bullet)$, $\text{Ho}(\blacksquare)$, and $\text{Tm}(\square)$.

The absence of any change of the spin configuration in $\text{PrFe}_{11}\text{Ti}$ enables us to establish that the value for the CEF parameter A_2^0 should obey $A_2^0 \leq -100$ K (Table I). For the values of A_2^0 larger than this value, a spin reorientation is calculated which is not corroborated by the experiments.

C. $\text{NdFe}_{11}\text{Ti}$

In $\text{NdFe}_{11}\text{Ti}$, a spin reorientation from a low-temperature cone structure to high-temperature c -axis anisotropy has been reported around 190–200 K.^{22,24}

Figure 4 shows the temperature dependence of the real χ' and imaginary χ'' components of the ac susceptibility of $\text{NdFe}_{11}\text{Ti}$. The pronounced anomalies just below 200 K are indicative of a second-order phase transition. The temperature of the phase transition, defined as the temperature where the first derivative of χ' reaches a minimum, is found to be 189 K. Since above this temperature $\text{NdFe}_{11}\text{Ti}$ exhibits uniaxial anisotropy, the occurrence of a second-order phase transition necessarily implies that a magnetic cone structure becomes stable below the spin-reorientation temperature. Less pronounced anomalies are found in χ' and χ'' around 240 K. In order to investigate the physical origin of this behavior, the ac susceptibility was measured on magnetically aligned $\text{NdFe}_{11}\text{Ti}$, with the field applied parallel or per-

TABLE I. The CEF parameters A_n^m and the R - T exchange field $2\mu_B B_{\text{exch}}$ (in units of K) and the magnetic moment of the Fe sublattice M_{Fe} (in units of $\mu_B/\text{f.u.}$) at 0 K for the RFe_{11}Ti series.

Compounds	$2\mu_B B_{\text{exch}}$	A_2^0	A_4^0	A_4^4	A_6^0	A_6^4	M_{Fe}
$\text{PrFe}_{11}\text{Ti}$	750	-100	0	0	0	0	19.30
$\text{NdFe}_{11}\text{Ti}$	600	-90	-160	120	60	0	19.30
$\text{SmFe}_{11}\text{Ti}$	460	-260	0	0	800	0	20.30
$\text{TbFe}_{11}\text{Ti}$	335	-49	-55	85	135	0	20.20
$\text{DyFe}_{11}\text{Ti}$	320	-45	-50	80	120	0	20.10
$\text{HoFe}_{11}\text{Ti}$	310	-42	-35	40	100	0	19.80
$\text{ErFe}_{11}\text{Ti}$	300	-40	-30	30	90	0	19.60
$\text{TmFe}_{11}\text{Ti}$	290	-30	-40	50	90	0	19.40

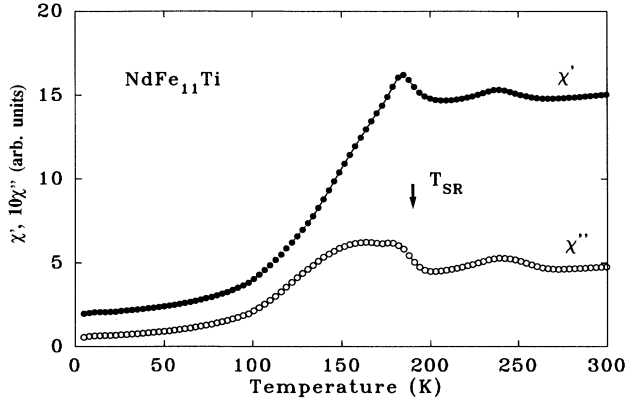


FIG. 4. Temperature dependence of χ' (●) and χ'' (○) of $\text{NdFe}_{11}\text{Ti}$.

pendicular to the alignment direction. In this experiment it was found that the anomalous behavior is most pronounced if the field is applied parallel to the alignment direction. From this, it can be concluded that the anomalous behavior is due to domain-wall motion excited by the ac field. This will be discussed in more detail in the section on $\text{TmFe}_{11}\text{Ti}$.

At 4.2 K, the magnetization of magnetically aligned $\text{NdFe}_{11}\text{Ti}$ (Fig. 6) exhibits anomalous behavior in the low-field region if it is measured with the field parallel to the alignment direction. This anomalous behavior becomes more manifest if the first derivative of the magnetization is considered (see inset in Fig. 6). This suggests that this phenomenon is associated with a FOMP. As described earlier,²⁵ the value of the critical field B_{cr} of the FOMP is given by the maximum of dM/dB , which in the present measurement on $\text{NdFe}_{11}\text{Ti}$ is located at 3.2 T. The temperature dependences of B_{cr} and of the anisotropy field B_a in $\text{NdFe}_{11}\text{Ti}$ have been measured by means of the SPD technique. The temperature dependences of B_{cr} and B_a are given in Fig. 5. The FOMP transitions, which are easily observed below 150 K, have been measured with the field applied parallel to the c axis. It is interest-

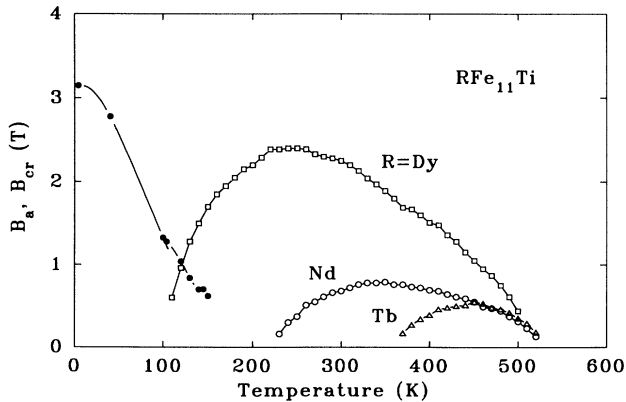


FIG. 5. Temperature dependence of the anisotropy field B_a of $R\text{Fe}_{11}\text{Ti}$ with $R = \text{Nd}$ (○), Tb (△), and Dy (□) and the critical field of FOMP B_{cr} of $\text{NdFe}_{11}\text{Ti}$ (●).

ing to note that this is the first compound of the $R(\text{Fe},\text{M})_{12}$ type in which a FOMP is observed with the field applied along the c direction. The magnetization curves for the field applied along various crystallographic directions, calculated with the CEF parameters and with the value for the exchange field tabulated in Table I, are shown in Fig. 6. The experimentally observed anomaly in the magnetization is found as a FOMP transition of type I¹³ in the magnetization for the field along the [001] direction. The calculated value of B_{cr} equals 2.7 T which, considering the presence of a demagnetizing field, is in good agreement with the experimental value of 3.2 T. The calculated value for the spin-reorientation temperature T_{SR} equals 187 K and the calculated zero-temperature value for the cone angle θ_c between the EMD and the c axis equals 53.9° (Fig. 21 and Table II).

D. $\text{SmFe}_{11}\text{Ti}$

Magnetization measurements on a $\text{SmFe}_{11}\text{Ti}$ single crystal by Kaneko *et al.*¹ at temperatures between 4.2 and 293 K have demonstrated that below 100 K the magnetization measured with the field applied perpendicular to the c axis exhibits an anomalous increase. In agreement with this, Li *et al.*,²⁶ Hu *et al.*,²⁷ and Hu *et al.*²² observed anomalous magnetization behavior in magnetically aligned samples. These later authors have claimed that a type-II FOMP occurs in $\text{SmFe}_{11}\text{Ti}$.

The temperature dependence of the ac susceptibility measured on polycrystalline $\text{SmFe}_{11}\text{Ti}$ is shown in Fig. 3. There is no spin reorientation expected in this compound. However, around 200 K a very slight anomaly may be distinguished, which becomes much more pronounced if the measurement is repeated on a magnetically aligned sample where the ac field is applied parallel to the alignment direction (Fig. 7). Since a temperature-induced spin reorientation in $\text{SmFe}_{11}\text{Ti}$ is unlikely in view of the same

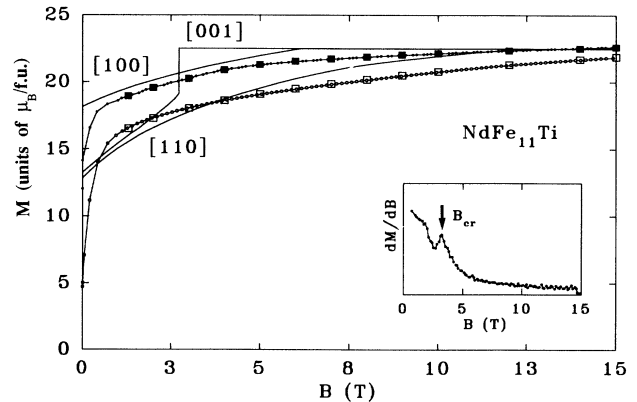


FIG. 6. High-field magnetization of 4.2 K of magnetically aligned $\text{NdFe}_{11}\text{Ti}$ with the field applied parallel (■) and perpendicular (□) to the alignment direction. The large and small dots represent the measurements obtained by employing “stepwise” and “continuous” field pulses. The inset shows the dM/dB vs B . The solid line is the calculated magnetization curve for single-crystalline $\text{NdFe}_{11}\text{Ti}$.

TABLE II. Magnetic properties of $R\text{Fe}_{11}\text{Ti}$ compounds, B_a is the magnetocrystalline anisotropy field and B_{cr} the critical field of FOMP (in units of T). T_{SR} is the spin-reorientation temperature (in units of K). θ_c is the cone angle, the angle between the EMD and the c axis.

Compound	B_a^{expt}		B_{cr}^{expt} (4.2 K)	B_{cr}^{clac} (0 K)	T_{SR}^{expt}	T_{SR}^{clac}	θ_c^{clac}
	(4.2 K)	(300 K)					
YFe_{11}Ti	4.05	2.23					
$\text{NdFe}_{11}\text{Ti}$		0.66	3.2	2.7 [001]	189	187	53.9° (0 K)
$\text{SmFe}_{11}\text{Ti}$		9.90					
$\text{GdFe}_{11}\text{Ti}$	5.93	3.92					
$\text{TbFe}_{11}\text{Ti}$					339	340	90.0° (0 K)
$\text{DyFe}_{11}\text{Ti}$		2.25			98	98	40.9° (98 K)
							90.0° (0 K)
					214	218	
$\text{HoFe}_{11}\text{Ti}$		2.83	2.6	3.2 [110] 2.4 [100]			
$\text{ErFe}_{11}\text{Ti}$		2.83	7.5	7.0 [110] 9.7 [100]	48	47	21.2° (0 K)
$\text{TmFe}_{11}\text{Ti}$		2.28	6.4	6.6 [110] 9.4 [100]			

EMD's of the Sm and the Fe sublattices, the anomaly around 200 K probably has a different physical origin, possibly similar to the anomaly observed in $\text{NdFe}_{11}\text{Ti}$ around 240 K.

The temperature dependence of B_a for $\text{SmFe}_{11}\text{Ti}$ determined by the SPD technique is shown in Fig. 8. Compared to the other $R\text{Fe}_{11}\text{Ti}$ compounds (Figs. 6 and 12), the values of B_a in $\text{SmFe}_{11}\text{Ti}$ are fairly large. Figure 9 shows the high-field magnetization measurement on magnetically aligned $\text{SmFe}_{11}\text{Ti}$ at 4.2 K with the field applied parallel or perpendicular to the alignment direction. An anomalous increase of the magnetization occurs around 10.5 T for the field applied perpendicular to the alignment direction. For comparison, the results obtained by Kaneko *et al.*¹ on a single crystal have also been included in Fig. 9. The temperature dependence of the critical field B_s , the field where the magnetization increases fastest, can also be determined by means of the SPD technique (Fig. 8). It must be noted that, on the basis of the

available experimental data, it is not possible to decide whether the transition in the magnetization is first or second order. The CEF calculations on $\text{SmFe}_{11}\text{Ti}$ carried out by Hu *et al.*,²⁸ Moze *et al.*,²⁹ and Kaneko *et al.*¹ lead to magnetization curves in which no discontinuous jump in the magnetization is seen, suggesting that this field-induced transition is not first order.

The CEF parameters for $\text{SmFe}_{11}\text{Ti}$ tabulated in Table I have been deduced by fitting calculated magnetization curves in the temperature interval from 4.2 to 293 K to the single-crystal results of Kaneko *et al.*¹ In the calculations, only one minimum in the free energy $F(T, \mathbf{B}, \mathbf{B}_{\text{exch}})$ is found for different directions in fields up to 40 T and at all considered temperatures. Therefore, it can be concluded that in $\text{SmFe}_{11}\text{Ti}$ no FOMP transition, but a continuous rotation of the magnetic moments (possibly a SOMP³⁰) takes place in the external field. In Fig. 9, the calculated magnetization curves at 0 K for a single-crystalline $\text{SmFe}_{11}\text{Ti}$ with fields applied along the

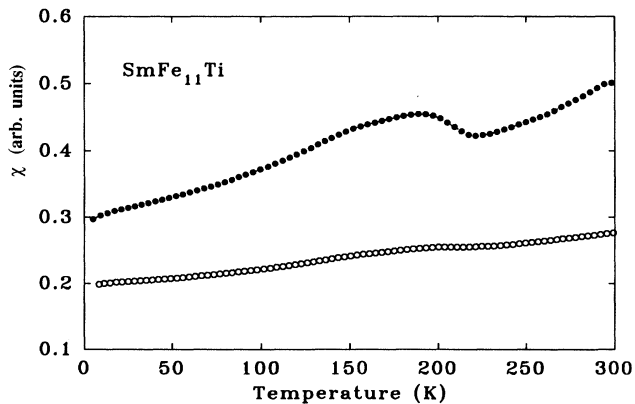


FIG. 7. Temperature dependence of χ' measured on magnetically aligned $\text{SmFe}_{11}\text{Ti}$ with the ac field applied parallel (●) and perpendicular (○) to the alignment direction.

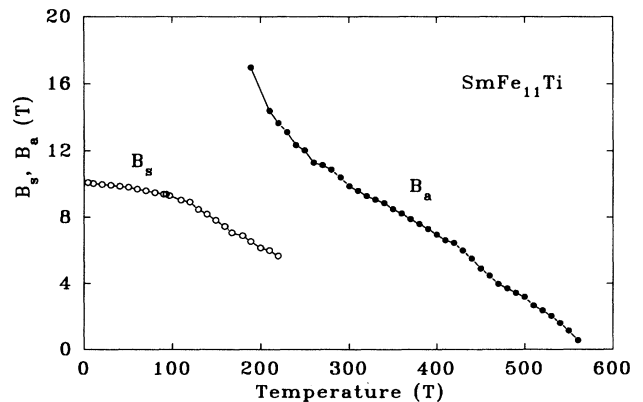


FIG. 8. Temperature dependence of the anisotropy field, B_a , (●) and the critical field of the “anomalous increase” of the magnetization, B_s , (○) of $\text{SmFe}_{11}\text{Ti}$.

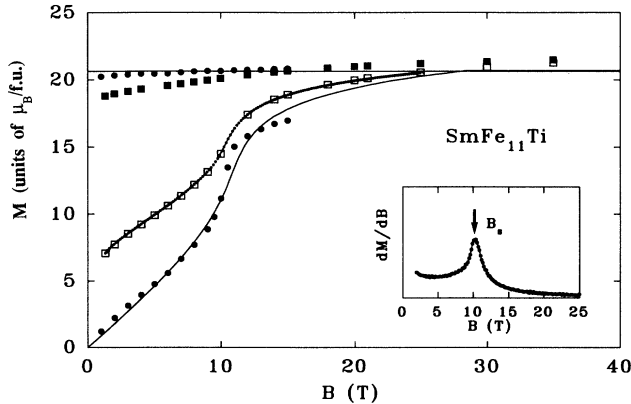


FIG. 9. High-field magnetization at 4.2 K of magnetically aligned $\text{SmFe}_{11}\text{Ti}$ with the field applied parallel (\blacksquare) and perpendicular (\square) to the alignment direction. The large and small dots represent the measurements obtained by employing “stepwise” and “continuous” field pulses. The inset shows the dM/dB vs B . The solid line is the calculated magnetization curve for single-crystalline $\text{SmFe}_{11}\text{Ti}$. The magnetization measurements on single-crystalline $\text{SmFe}_{11}\text{Ti}$ (\bullet) at 4.2 K are plotted for comparison.¹

[001] and [100] directions are shown (solid line in Fig. 9). The CEF parameters and the value of B_{exch} in $\text{SmFe}_{11}\text{Ti}$ in Table I are in reasonable agreement with the values reported by Kaneko *et al.*¹ ($A_2^0 = -252$ K, $A_4^0 = 60$ K, $A_6^0 = 940$ K, and $2\mu_B B_{\text{exch}} = 480$ K) and by Hu *et al.*,²⁸ and Moze *et al.*²⁹ ($A_2^0 = -257$ K, $A_4^0 = 72$ K, $A_6^0 = 1180$ K, and $2\mu_B B_{\text{exch}} = 474$ K). In Table I, it can be seen that the absolute values of A_2^0 and A_6^0 for $\text{SmFe}_{11}\text{Ti}$ are extremely large compared with the values for the other compounds. A similar behavior for the A_6^0 parameter is found for $\text{Sm}_2\text{Fe}_{14}\text{B}$ in the $R_2\text{Fe}_{14}\text{B}$ series.³¹ At present, we are not able to explain this.

E. $\text{TbFe}_{11}\text{Ti}$

Hu *et al.*^{22,39} have reported two spin reorientations to occur in $\text{TbFe}_{11}\text{Ti}$ at 230 and 450 K. They propose a complex magnetic structure to be stable below 230 K, planar anisotropy between 230 and 450 K and uniaxial anisotropy above 450 K. However, they do not succeed in describing the proposed temperature variation of the EMD in $\text{TbFe}_{11}\text{Ti}$ in their CEF calculations.^{5,28} Zhang *et al.* have reported only one spin reorientation in $\text{TbFe}_{11}\text{Ti}$ at 285 K in Ref. 32 (at 330 K in Ref. 33).

The temperature dependence of the ac susceptibility of $\text{TbFe}_{11}\text{Ti}$ does not indicate any spin orientation occurring below 300 K (Fig. 3). Therefore, we also measured the temperature dependence of the magnetization up to 650 K in various applied fields (0.01, 0.1, 0.5, 1.0, and 2.3 T). Clear evidence for a spin reorientation is found which, being strongly field dependent, occurs at temperatures ranging between 339 K in 0.01 T and 270 K in 2.3 T (Fig. 10). The peaklike shape of the anomaly, being similar to that found in low-field measurements on $\text{Er}_2\text{Fe}_{14}\text{B}$, is indicative of a first-order transition.

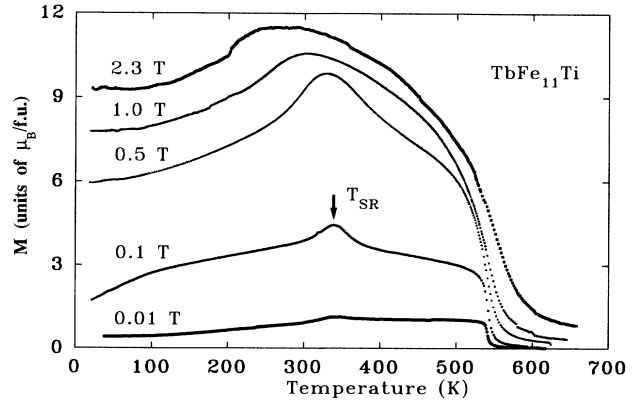


FIG. 10. Temperature dependence of the magnetization of $\text{TbFe}_{11}\text{Ti}$ in different external fields.

The temperature dependence of B_a for $\text{TbFe}_{11}\text{Ti}$ has been determined by the SPD technique and is shown in Fig. 5. The SPD peak, corresponding with the anisotropy field, could only be detected above 340 K. Its absence below 340 K can be understood in terms of a change of the EMD from the c axis at higher temperatures to the basal plane at low temperatures.

On the basis of the above experimental results, the spin-reorientation transition in $\text{TbFe}_{11}\text{Ti}$ is expected to have a different physical nature as in $\text{NdFe}_{11}\text{Ti}$. In the case of $\text{TbFe}_{11}\text{Ti}$, it is attributed to the temperature-induced competition of the uniaxial Fe-sublattice anisotropy and the planar Tb-sublattice anisotropy.

From CEF calculations, in which the parameters tabulated in Table I are used, it follows that the difference in value of the Tb and Fe-sublattice anisotropy energies is fairly small around room temperature. Therefore, the spin-reorientation temperature is very sensitive to the magnitude of the applied field and to the crystallographic directions along which the field is applied. The experiments by Hu *et al.*²² and Zhang *et al.*^{32,33} were all performed in relatively high fields. It may be concluded that the lowest spin-reorientation temperature reported by Zhang *et al.*³² is due to the application of too high a magnetic field before and during the measurement.

Due to the very small difference in the value of the Tb- and Fe-sublattice anisotropy energies above 300 K, it is difficult to describe the spin reorientation of $\text{TbFe}_{11}\text{Ti}$ by the model described in Sec. III. With the CEF parameters listed in Table I, extrapolated from the rest of the heavy rare-earth compounds, the calculated T_{SR} for $\text{TbFe}_{11}\text{Ti}$ is 340 K. However, in the calculation it is found that, in a temperature range from about 300 to 340 K, the EMD changes a number of times with temperature between the c axis and the basal plane, which is contradictory to the experiment. Interestingly enough, this behavior is also found even if only the second-order CEF parameter is taken into account. In order to overcome this shortcoming originating from the model itself, a slightly smaller value of $|A_2^0|$ should be taken above T_{SR} . Below T_{SR} a slightly higher value of $|A_2^0|$ (combining with the value listed in Table I) is necessary. It is

worthwhile to note that a temperature dependence of A_n^m was also proposed in the CEF analysis of the systems $R\text{Co}_5$ ($R = \text{Nd, Sm}$),^{34,35} $R_2\text{Co}_{14}\text{B}$ ($R = \text{Pr, Nd}$),³⁶ $\text{Nd}_2\text{Fe}_{14}\text{C}$.³⁷ However, the physical origin of this change as yet remains unclear.

F. DyFe₁₁Ti

The magnetization of a DyFe₁₁Ti single crystal has been investigated in the temperature range from 4.2 to 300 K and the results have been analyzed in terms of a CEF calculation.^{5,22,28,38} The EMD changes from c axis at T_{SR1} of about 200 K via a cone to basal plane at T_{SR2} of about 100 K. However, Andreev *et al.*⁴ have reported that at 4.2 K the EMD still deviates about 10° from the basal plane. Additionally, for T_{SR2} different temperatures like 58 K and 100 K are reported.^{5,22} Below 100 K, a FOMP transition was detected along the [100], [001], and [110] directions in low fields (below 1 T).^{4,5}

Figure 11 shows the temperature dependence of χ' and χ'' for DyFe₁₁Ti. At 214 K, the temperature corresponding to the minimum of $d\chi'/dT$, a spin-reorientation transition of the second order from c axis to cone is detected. At 98 K, a kink is observed, corresponding to a first-order transition from cone to basal plane. As mentioned before for TbFe₁₁Ti, the spin-reorientation temperature is very sensitive to the magnitude of the external field and also to the crystallographic direction along which the external field is applied. With the CEF parameters and the value of the exchange field listed in Table I, the spin-orientation temperatures, $T_{\text{SR1}} = 218$ K and $T_{\text{SR2}} = 98$ K, could be calculated for DyFe₁₁Ti. Furthermore, the CEF calculation shows that application of an external field of 0.3 T along the c axis depresses the values for T_{SR1} and T_{SR2} to 202 and 61 K, respectively. In this way, we can understand the low values for T_{SR1} (200 K) and T_{SR2} (58 K) derived by Hu *et al.*⁵ from the temperature dependence for the magnetization in a field of 0.5 T applied along the c axis of DyFe₁₁Ti. After correction for the demagnetizing field, the internal field amounts to approximately 0.3 T. Hu *et al.*⁵ determined the following set of

the CEF parameters for DyFe₁₁Ti: $A_2^0 = -50$ K, $A_4^0 = -149$ K, $A_4^4 = 170$ K, $A_6^0 = 247$ K, and $A_6^4 = 5.5$ K. Only the second-order CEF parameter is in good agreement with the value obtained in the present investigation (Table I). The absolute values of the fourth- and sixth-order CEF parameters of Hu *et al.* are all two or three times larger than in the present investigation. This disagreement is caused by the neglect of the effect of the applied field on the spin-reorientation temperature by Hu *et al.*⁵

The temperature dependence of B_a of DyFe₁₁Ti is shown in Fig. 6. B_a has a maximum at about 220 K, where the spin reorientation from c axis to cone occurs, and is about zero at 100 K, the temperature where the transition from cone to plane takes place. The observed temperature dependence of B_a is in good agreement with the EMD changes deduced from the ac susceptibility.

G. HoFe₁₁Ti

Boltich *et al.*,⁴⁰ Sinha *et al.*,⁴¹ and Zhang *et al.*³³ claim a spin-reorientation transition in HoFe₁₁Ti at about 50 K from a high-temperature easy c -axis spin configuration to a cone structure. In contrast with this, many others, e.g., Hu *et al.*^{22,28} and Yang *et al.*⁴² have pointed out that the EMD of HoFe₁₁Ti remains easy c axis down to the lowest temperatures. Hu *et al.*²⁷ have observed a FOMP transition at 77 K at a field of 1.89 T.

The temperature dependence of χ' for HoFe₁₁Ti is shown in Fig. 3. There is no clear indication for a spin reorientation in this compound. This conclusion is confirmed by the observed temperature dependences of the anisotropy field B_a and of the FOMP field B_{cr} (Fig. 12). The large difference in value of B_a and B_{cr} around 160 K, the onset temperature of the FOMP, indicates that the FOMP is of type II. Figure 13 shows, as an example, the experimental SPD curve of HoFe₁₁Ti at 4.2 K. The value of B_{cr} of 2.64 T is given by the field where $d^2M/dB^2 = 0$.¹⁶ The high-field magnetization measurement on magnetically aligned HoFe₁₁Ti at 4.2 K is shown

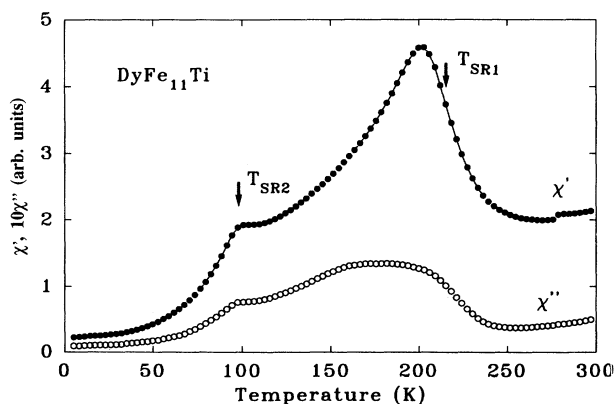


FIG. 11. Temperature dependence of χ' (●) and χ'' (○) of DyFe₁₁Ti.

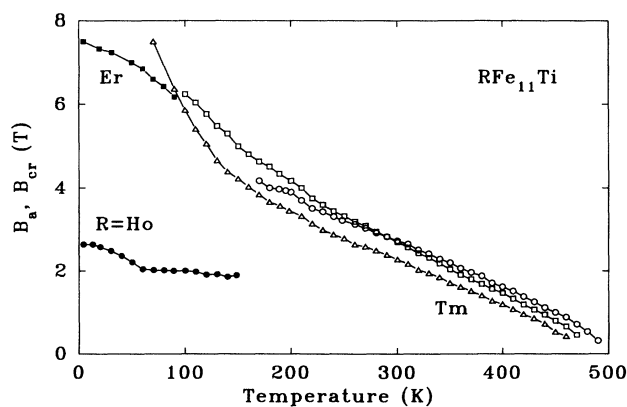


FIG. 12. Temperature dependence of the anisotropy field, B_a , of $R\text{Fe}_{11}\text{Ti}$ with $R = \text{Ho}$ (○), Er (□), and Tm (△) and the critical field for the FOMP B_{cr} for $R\text{Fe}_{11}\text{Ti}$ with $R = \text{Ho}$ (●) and Er (■).

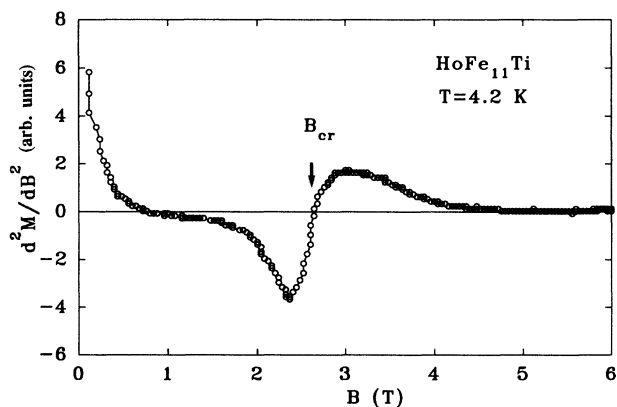


FIG. 13. A typical SPD signal of the FOMP transition for $\text{HoFe}_{11}\text{Ti}$ at 4.2 K.

in Fig. 14. Also in this measurement, a FOMP transition is clearly detected when the field is applied perpendicular to the alignment direction. The value of B_{cr} , determined as the field where dM/dB achieves a maximum value, is 2.6 T. The values of B_{cr} , calculated by means of the CEF parameters given in Table I, are 2.4 T for B along the [100] direction and 3.2 T along the [110] direction. The magnetization curves calculated for single-crystalline $\text{HoFe}_{11}\text{Ti}$ are also shown in Fig. 14.

H. $\text{ErFe}_{11}\text{Ti}$

In $\text{ErFe}_{11}\text{Ti}$, a change of EMD has been detected at about 50 K from the c axis above this temperature to a cone at lower temperatures.²² Hu *et al.*²⁷ report a FOMP transition at 4.54 T at 77 K.

Figure 15 shows the temperature dependences of χ' and χ'' of $\text{ErFe}_{11}\text{Ti}$ in which a spin-reorientation transi-

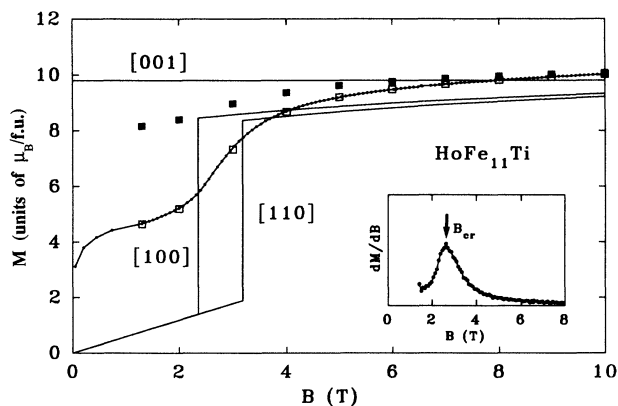


FIG. 14. High-field magnetization at 4.2 K of magnetically aligned $\text{HoFe}_{11}\text{Ti}$ with the field applied parallel (■) and perpendicular (□) to the alignment direction. The large and small dots represent the measurements obtained by employing “stepwise” and “continuous” field pulses. The inset shows the dM/dB vs B . The solid line is the calculated magnetization curve for single-crystalline $\text{HoFe}_{11}\text{Ti}$.

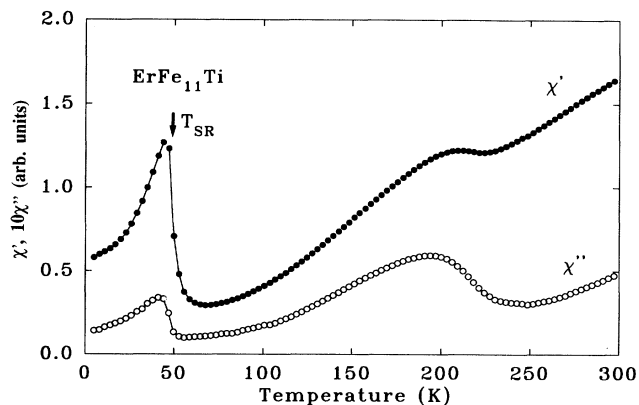


FIG. 15. Temperature dependence of χ' (●) and χ'' (○) of $\text{ErFe}_{11}\text{Ti}$.

tion of second order, is seen at 48 K, where the first derivative of χ' has its minimum. Anomalous behavior of χ' and χ'' , similar to what is observed in $\text{NdFe}_{11}\text{Ti}$ and $\text{SmFe}_{11}\text{Ti}$, is found around 210 K. Figure 16 shows the temperature dependence of χ' measured on magnetically aligned $\text{ErFe}_{11}\text{Ti}$. As in $\text{NdFe}_{11}\text{Ti}$ and $\text{SmFe}_{11}\text{Ti}$, the high-temperature anomaly is enhanced when the ac field is applied parallel to the alignment direction and strongly suppressed when it is perpendicular to the alignment direction.

The temperature dependences of the anisotropy field B_a and the critical field of the FOMP B_{cr} for $\text{ErFe}_{11}\text{Ti}$ as determined with the SPD technique are shown in Fig. 12. The observation that around 100 K the values for B_a and B_{cr} are about the same indicates that the FOMP, which is observable below 100 K, is of type I. In the magnetization at 4.2 K, shown in Fig. 17, the FOMP can be detected at 7.6 T, the field where the first derivative of the magnetization has a maximum (see inset in Fig. 17). This value is in fair agreement with the value of 7.5 T obtained by the SPD technique. The occurrence of both a spin reorientation and a FOMP in $\text{ErFe}_{11}\text{Ti}$ suggests that the

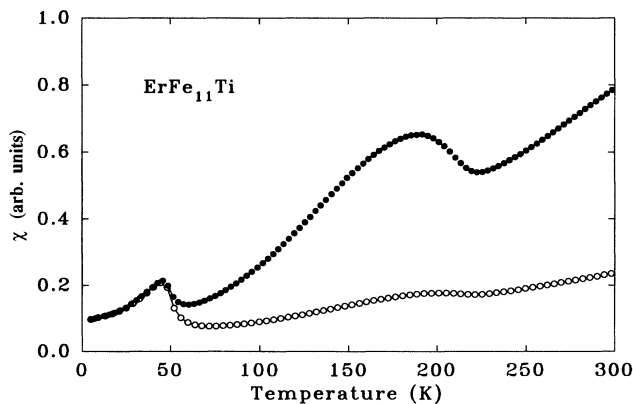


FIG. 16. Temperature dependence of χ' measured on magnetically aligned $\text{ErFe}_{11}\text{Ti}$ with the ac field applied parallel (●) and perpendicular (○) to the alignment direction.

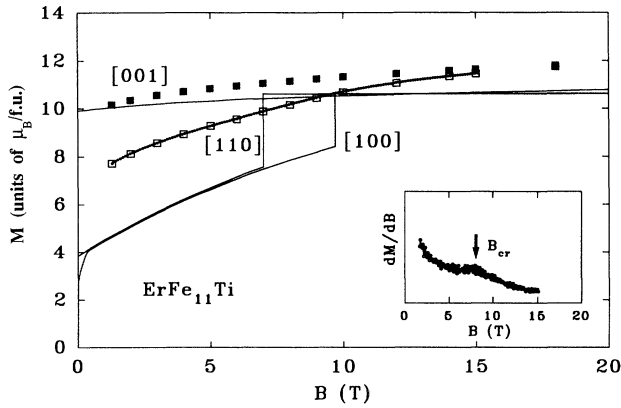


FIG. 17. High-field magnetization at 4.2 K of magnetically aligned $\text{ErFe}_{11}\text{Ti}$ with the field applied parallel (■) and perpendicular (□) to the alignment direction. The large and small dots represent the measurements obtained by employing “stepwise” and “continuous” field pulses. The solid line is the calculated magnetization curve for single-crystalline $\text{ErFe}_{11}\text{Ti}$.

high-order CEF terms play a key role in determining the EMD of the Er sublattice. The situation found for $\text{ErFe}_{11}\text{Ti}$ is very similar to that for the well-known $\text{Nd}_2\text{Fe}_{14}\text{B}$ compound, which exhibits a spin reorientation (c axis to cone) at 135 K⁴³ and a type-I FOMP below 220 K.^{16,31,44–46} The cone angle in $\text{ErFe}_{11}\text{Ti}$ is calculated to be 21° at 0 K, the spin-reorientation temperature 47 K, and the critical field for the FOMP 6.9 T for the field along the [110] direction and 9.7 T along the [100] direction, which is in good agreement with the experiments. The calculated magnetization curves for single-crystalline $\text{ErFe}_{11}\text{Ti}$ are also shown in Fig. 17.

I. $\text{TmFe}_{11}\text{Ti}$

According to Hu *et al.*,²² no spin reorientation takes place in this compound. The EMD of $\text{TmFe}_{11}\text{Ti}$ remains parallel to the c axis at all ferrimagnetically ordered temperatures.

The temperature dependences of χ' measured on polycrystalline $\text{TmFe}_{11}\text{Ti}$ are shown in Fig. 3. Around 200 K, a broad anomaly can be distinguished. In order to find out whether this anomaly is due to a spin reorientation, the temperature dependence of χ' was also measured on magnetically aligned $\text{TmFe}_{11}\text{Ti}$, both with the field parallel and perpendicular to the alignment direction (Fig. 18). Similar to what was found for $\text{NdFe}_{11}\text{Ti}$, $\text{SmFe}_{11}\text{Ti}$, and $\text{ErFe}_{11}\text{Ti}$, the anomaly is strongly reduced when the ac field is applied perpendicular to the alignment direction and it is enhanced if it is applied parallel to the alignment direction.

The anisotropy field B_a of $\text{TmFe}_{11}\text{Ti}$ could be determined by the SPD technique from about 60 K up to the Curie temperature (Fig. 12). Below 60 K, the SPD signal becomes unclear due to noise. Because the SPD signal was detected on polycrystalline material above room temperature, it can be concluded that the EMD of $\text{TmFe}_{11}\text{Ti}$

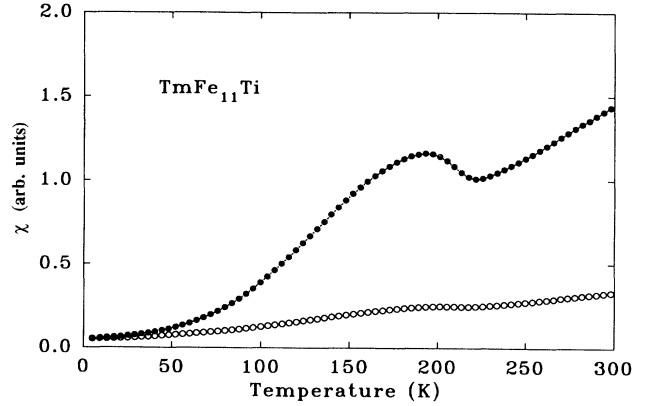


FIG. 18. Temperature dependence of χ' measured on magnetically aligned $\text{TmFe}_{11}\text{Ti}$ with the ac field applied parallel (●) and perpendicular (○) to the alignment direction.

is parallel to the c axis at these temperatures. The smooth variation of B_a on going to temperatures below room temperature shows that the anisotropy remains uniaxial down to at least 60 K.

Figure 19 shows the high-field magnetization of $\text{TmFe}_{11}\text{Ti}$ at 4.2 K measured on aligned powder. A slightly anomalous magnetization behavior, likely to be associated with a FOMP, is observed if the field is applied perpendicular to the alignment direction. By means of the first derivative of the magnetization, the critical field of this FOMP was determined to be 6.4 T (see inset in Fig. 19).

In view of the above experimental results, we can conclude that the anomaly in the ac susceptibility observed in $\text{TmFe}_{11}\text{Ti}$ around 200 K, as well as the similar anomalies found in $\text{NdFe}_{11}\text{Ti}$, $\text{SmFe}_{11}\text{Ti}$, and $\text{ErFe}_{11}\text{Ti}$, are neither connected with a spin reorientation nor due to an impurity phase. The observation that the anomalous

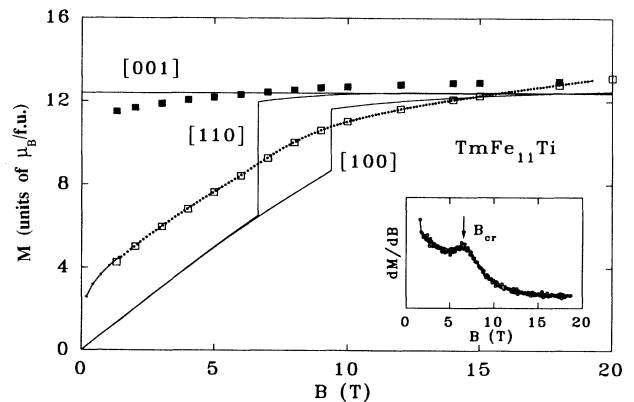


FIG. 19. High-field magnetization of 4.2 K of magnetically aligned $\text{TmFe}_{11}\text{Ti}$ with the field applied parallel (■) and perpendicular (□) to the alignment direction. The large and small dots represent the measurements obtained by employing “stepwise” and “continuous” field pulses. The inset shows the dM/dB vs B . The solid line is the calculated magnetization curve for single-crystallization $\text{TmFe}_{11}\text{Ti}$.

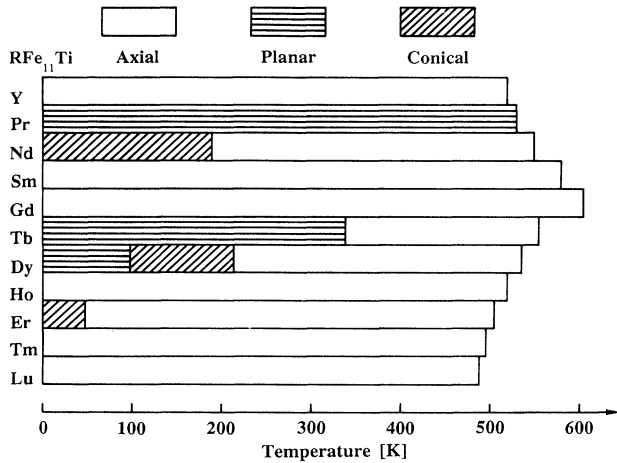


FIG. 20. Anisotropy diagram of the $RFe_{11}Ti$ series.

behavior is enhanced if the field is applied parallel to the alignment direction suggests that it may be connected with domain-wall motion. It must be noted that the anomalous behavior described above is not restricted to the $RFe_{11}Ti$ compounds, the subject of the present paper. Similar behavior has also been found for compounds in several other systems, like R_2Fe_{17} ,⁴⁷ R_2Co_{17} ,^{48,49} $R_2T_{14}X$ ($T = Fe, Co$; $X = B, C$),^{16,46,50,51} which points to a more general physical origin which, however, is not yet understood.

The CEF calculations with the parameters listed in Table I, provide magnetization curves of $TmFe_{11}Ti$ as shown in Fig. 19. The critical field for the FOMP in $TmFe_{11}Ti$ is calculated to be 6.6 T for the field along the [110] direction and 9.4 T for the [100] direction.

V. SUMMARY AND CONCLUSIONS

In the present paper, a systematic study of $RFe_{11}Ti$ compounds has been presented by means of a variety of magnetic measurements. The temperature dependence of the ac susceptibility was used to detect magnetic phase transitions and the SPD technique to determine the anisotropy field and the critical field for the FOMP. Magnetization measurements were carried out in high fields to determine the magnetization behavior of these strongly anisotropic materials and to observe the FOMP transitions, and in low fields to investigate spin reorientations above room temperature and to determine the Curie temperatures. Spin reorientations were detected in the compounds with $R = Nd, Tb, Dy$, and Er . In the compounds with $R = Nd, Ho, Er, Tm$, a FOMP transition was found at low temperatures. The anomalous increase of magnetization found in $SmFe_{11}Ti$ if the external field is applied

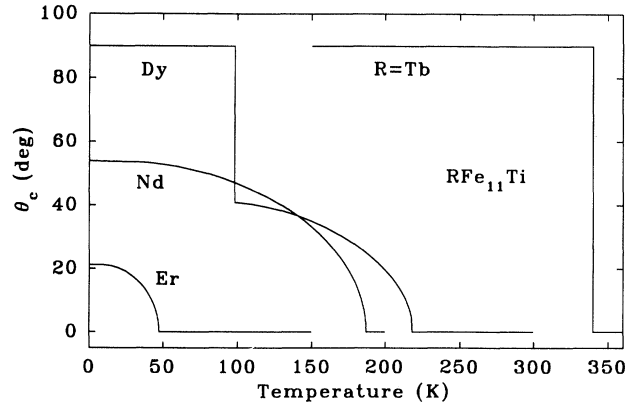


FIG. 21. The calculated temperature dependence of the cone angle, θ_c , of $RFe_{11}Ti$ with $R = Nd, Tb, Dy$, and Er .

perpendicular to the alignment direction, is shown not to be a FOMP. A diagram, representing the variation of the EMD with temperature for each $RFe_{11}Ti$ compound, is presented (Fig. 20).

The observed spin reorientations and FOMP transitions, as well as the magnetocrystalline anisotropy of the $RFe_{11}Ti$ compounds, have been analyzed in terms of the CEF interaction and the $R-T$ exchange interaction. A set of CEF parameters and the $R-T$ exchange fields has been derived (Table I). Similarly, as found in $R_2Fe_{14}B$ compounds,⁵² the CEF parameters vary only slightly from $R = Tb$ to Tm , suggesting that the magnetic behavior of heavy rare-earth compounds can be well described in terms of CEF calculation. However, this is not the case for the light rare-earth compounds. By means of the CEF parameters and the $R-T$ exchange fields listed in Table I, the temperature dependences of the cone angle θ_c for $RFe_{11}Ti$ compounds with $R = Nd, Tb, Dy$, and Er have been calculated (Fig. 21). The experimental and calculated values of the anisotropy field B_a , the critical field for the FOMP B_{cr} and the spin-reorientation temperature T_{SR} for the $RFe_{11}Ti$ compounds are compared (Table II).

ACKNOWLEDGMENTS

This work was supported by the "Fond zur Förderung der Wissenschaftlichen Forschung von Österreich" under Grant Nos. 7327, 7620 and P8913-PHY and the East-West Program, "Microcrystalline-amorphous magnetic materials" of the Austrian Ministry of Sciences and Research. We thank Lu Ping and Professor E. Gratz for performing the x-ray diffraction analysis, Professor G. Hilscher for very fruitful discussions, and Dipl. Ing. M. Forthuber for friendly help during the ac susceptibility measurements. One of the authors (X.C.K) thanks the Max-Planck Gesellschaft and the University of Dublin for financial support.

- *Present address: Max-Planck-Institut für Metallforschung, Institut für Physik, Heisenbergstrasse 1, 7000 Stuttgart 80, Germany. Permanent address: Institute of Metal Research, Academia Sinica, Shenyang 110015, China.
- †Permanent address: Department of Physics, Jilin University, Changchun 130023, China.
- ¹T. Kaneko, M. Yamada, K. Ohashi, T. Tawara, R. Osugi, H. Yoshida, G. Kido, and Y. Nakagawa, in *Proceedings of the 10th International Workshop on Rare Earth Magnets and Their Applications, Kyoto, Japan* (The Society of Nontraditional Metallurgy, Kyoto, Japan, 1989), p. 191.
- ²K. Ohashi, T. Yokoyawa, R. Osugi, and Y. Tawara, *IEEE Trans. Magn.* **MAG-23**, 3101 (1987).
- ³K. Ohashi, Y. Tawara, R. Osugi, and M. Shimao, *J. Appl. Phys.* **64**, 5714 (1988).
- ⁴A. V. Andreev, M. I. Bartashevich, N. V. Kundrevatykh, S. M. Razgonyaev, S. S. Sigaev, and E. N. Tarasov, *Physica B* **167**, 139 (1990).
- ⁵Bo-Ping Hu, Hong-Shuo Li, J. M. D. Coey, and J. P. Gavigan, *Phys. Rev. B* **41**, 2221 (1990).
- ⁶A. V. Andreev, V. Sechovsky, N. V. Kundrevatykh, S. S. Sigaev, and E. N. Tarasov, *J. Less-Common Met.* **144**, L21 (1988).
- ⁷K. Ohashi, Y. Tawara, and R. Osugi, *J. Less-Common Met.* **139**, L1 (1988).
- ⁸O. Moze, L. Pareti, M. Solzi, and W. I. F. David, *Solid State Commun.* **66**, 465 (1988).
- ⁹J. Ding and M. Rosenberg, *J. Magn. Magn. Mater.* **83**, 257 (1990).
- ¹⁰L. Schultz, K. Schnitzke, and J. Wecker, *J. Magn. Magn. Mater.* **83**, 254 (1990).
- ¹¹G. Asti and S. Rinaldi, *Phys. Rev. Lett.* **28**, 1584 (1972).
- ¹²G. Asti and S. Rinaldi, *J. Appl. Phys.* **45**, 3600 (1974).
- ¹³G. Asti and F. Bolzoni, *J. Magn. Magn. Mater.* **20**, 29 (1980).
- ¹⁴G. Asti, in *Ferromagnetic Materials*, edited by K. H. J. Buschow and E. P. Wohlfarth (North-Holland, Amsterdam, 1990), Vol. 5, p. 397.
- ¹⁵L. Pareti, *J. Phys. (Paris) Colloq.* **49**, C8-551 (1988).
- ¹⁶X. C. Kou and R. Grössinger, *J. Magn. Magn. Mater.* **95**, 184 (1991).
- ¹⁷The Ba-ferrite single crystal was provided by and the SQUID measurement were performed by Dr. F. Schumacher of the Institut für Werkstoffe der Elektrotechnik, Rhein.-Westl. Tech. Hochschule Aachen, Germany.
- ¹⁸R. Gersdorf, F. R. de Boer, J. C. Walfrat, F. A. Muller, and L. W. Roeland, in *High Field Magnetism*, edited by M. Date (North-Holland, Amsterdam, 1983), p. 277.
- ¹⁹L. W. Roeland, R. Gersdorf, and W. C. M. Mattens, *IEEE Trans. Magn.* **MAG-24**, 911 (1988).
- ²⁰L. W. Roeland, R. Gersdorf, and W. C. M. Mattern, *Physica B* **155**, 58 (1989).
- ²¹B. G. Wybourne, *Spectroscopic Properties of Rare Earths* (Interscience, New York, 1965).
- ²²Bo-Ping Hu, Hong-Shuo Li, J. P. Gavigan, and J. M. D. Coey, *J. Phys. Condens. Matter* **1**, 755 (1988).
- ²³J. M. D. Coey, *J. Magn. Magn. Mater.* **80**, 1 (1989).
- ²⁴M. Q. Huang, Y. Xu, S. G. Sankar, and W. E. Wallace, in *Proceedings of the 6th International Symposium on Magnetic Anisotropy and Coercivity in Rare Earth-Transition Metal Alloys*, edited by S. G. Sankar (Carnegie-Mellon University, Pittsburgh, 1990), p. 400.
- ²⁵X. C. Kou, T. S. Zhao, R. Grössinger, H. R. Kirchmayr, X. Li, and F. R. de Boer, *Phys. Rev. B* **46**, 11 204 (1992).
- ²⁶Hong-Shuo Li, Bo-Ping Hu, J. P. Gavigan, J. M. D. Coey, L. Pareti, and O. Moze, *J. Phys. (Paris) Colloq.* **49**, C8-541 (1988).
- ²⁷Jifan Hu, Tao Wang, Shougong Zhang, Yizhong Wang, and Zhenxi Wang, *J. Magn. Magn. Mater.* **74**, 22 (1988).
- ²⁸Bo-Ping Hu, thesis, Trinity University, Dublin, 1990 (unpublished).
- ²⁹O. Moze, R. Caciuffo, H.-S. Li, B.-P. Hu, J. M. D. Coey, R. Osborn, and A. D. Taylor, *Phys. Rev. B* **42**, 1940 (1990).
- ³⁰Zhao Tong, Sun Xiao-kai, Zhang Zhi-dong, Wang Qun, Y. C. Chuang, and F. R. de Boer, *J. Magn. Magn. Mater.* **104-107**, 2119 (1992).
- ³¹M. Yamada, H. Kato, H. Yamamoto, and Y. Nakagawa, *Phys. Rev. B* **38**, 620 (1988).
- ³²L. Y. Zhang, B. M. Ma, Y. Zheng, and W. E. Wallace, *J. Appl. Phys.* **70**, 6119 (1991).
- ³³L. Y. Zhang, E. B. Boltich, V. K. Sinha, and W. E. Wallace, *IEEE Trans. Magn.* **MAG-25**, 3303 (1989).
- ³⁴T. S. Zhao, H. M. Jin, G. H. Guo, X. F. Han, and H. Chen, *Phys. Rev. B* **43**, 8593 (1991).
- ³⁵T. S. Zhao, H. M. Jin, R. Grössinger, X. C. Kou, and H. R. Kirchmayr, *J. Appl. Phys.* **70**, 6134 (1991).
- ³⁶Y. Yan, T. S. Zhao, and H. M. Jin, *J. Phys. Condens. Matter* **3**, 195 (1991).
- ³⁷T. S. Zhao, X. C. Kou, R. Grössinger, and H. R. Kirchmayr, *J. Magn. Magn. Mater.* **104-107**, 1347 (1992).
- ³⁸Bo-Ping Hu, Hong-Shuo Li, and J. M. D. Coey, *Solid State Commun.* **66**, 133 (1988).
- ³⁹Bo-Ping Hu, Hong-Shuo Li, and J. M. D. Coey, *Hyperfine Interact.* **45**, 233 (1989).
- ⁴⁰E. B. Boltich, B. M. Ma, L. Y. Zhang, F. Pourarian, S. K. Malik, S. G. Sankar, and W. E. Wallace, *J. Magn. Magn. Mater.* **78**, 364 (1989).
- ⁴¹V. K. Sinha, S. K. Malik, D. T. Adroja, J. Elbicki, S. G. Sankar, and W. E. Wallace, *J. Magn. Magn. Mater.* **80**, 281 (1989).
- ⁴²Ying-Chang Yang, Lin-Shu Kong, Yuan-Bo Zha, Hong Sun, and Xie-Di Pei, *J. Phys. (Paris) Colloq.* **49**, C8-543 (1988).
- ⁴³D. Givord, H. S. Li, and R. Perrier de la Bâthie, *Solid State Commun.* **51**, 857 (1984).
- ⁴⁴L. Pareti, F. Bolzoni, and O. Mose, *Phys. Rev. B* **32**, 7604 (1985).
- ⁴⁵F. Bolzoni, O. Mose, and L. Pareti, *J. Appl. Phys.* **62**, 615 (1987).
- ⁴⁶R. Grössinger, X. C. Kou, R. Krewenka, H. R. Kirchmayr, and M. Tokunaga, *IEEE Trans. Magn.* **MAG-26**, 1954 (1990).
- ⁴⁷X. C. Kou, T. S. Zhao, F. R. de Boer, and S. Hiroswawa (unpublished).
- ⁴⁸X. C. Kou, R. Grössinger, and G. Wiesinger, *J. Magn. Magn. Mater.* **104-107**, 1339 (1992).
- ⁴⁹X. C. Kou, T. S. Zhao, R. Grössinger, and F. R. de Boer, *Phys. Rev. B* **46**, 6225 (1992).
- ⁵⁰X. C. Kou, thesis, Techn. Universität, Vienna, 1991 (unpublished).
- ⁵¹X. C. Kou, R. Grössinger, and H. R. Kirchmayr, *J. Appl. Phys.* **70**, 6372 (1991).
- ⁵²T. S. Zhao, H. M. Jin, and Y. Zhu, *J. Magn. Magn. Mater.* **79**, 159 (1989).